Journal of Applied Polymer Science

The dominant factor for mechanical property of polyimide films containing heterocyclic moieties: In-plane orientation, crystallization, or hydrogen bonding

Longbo Luo,[1] Jing Zhang,[2] Jieyang Huang,[1] Yan Feng,[1] Chaorong Peng,[2] Xu Wang,[1] Xiangyang Liu[1]

[1]State Key Laboratory of Polymer Material and Engineering, College of Polymer Science and Engineering, Sichuan University, Chengdu 610065, People's Republic of China

[2]Radiation Chemistry Department, Sichuan Institute of Atomic Energy, Chengdu 610065, People's Republic of China

Correspondence to: X. Liu (E-mail: lxy6912@sina.com) and X. Wang (E-mail: wx2010_fight@163.com)

ABSTRACT: Crystallization, in-plane orientation, and hydrogen bonding interactions are three vital factors for enhancing mechanical properties of polyimide (PI) films. However, which is the dominant factor? In this study, three PI films containing heterocyclic moiety, poly(benzoxazole-imide), poly(benzimidazole-imide), and poly(pyrimidine-imide) were chosen to comparative study. The crystallinity of poly(benzoxazole-imide), poly(benzimidazole-imide), and poly(pyrimidine-imide) PI films are 36, 24, and 15%, respectively. The results of small angle X-ray scattering indicate poly(benzoxazole-imide) and poly(benzimidazole-imide) films show periodical lamellar structures, while poly(pyrimidine-imide) shows no long period due to low crystallinity. In-plane orientation (P_{200}) is calculated from polarized attenuated total reflection (ATR)-Fourier transform infrared and refractive indices. The order of in-plane orientation is poly(benzimidazole-imide) < poly(benzoxazole-imide) < poly(pyrimidine-imide). Hydrogen bonding interactions, which restrict chain motion and hinder spontaneous in-plane orientation, are only formed in poly(benzimidazole-imide). The relationship between mechanical properties and three influence factors are discussed, and the order of influence extent for mechanical properties of PI films is hydrogen bonding interactions < degree of crystallization < in-plane orientation. Two structure models for PI films are proposed in order to further confirm the dominant effect of in-plane orientation on the mechanical properties. © 2016 Wiley Periodicals, Inc. J. Appl. Polym. Sci. **2016**, *133*, 44000.

KEYWORDS: crystallization; mechanical properties; polyimides; structure–property relations

Received 15 April 2016; accepted 1 June 2016

DOI: 10.1002/app.44000

INTRODUCTION

Aromatic polyimides (PIs) are well known as high performance polymers due to their excellent thermal and thermooxidative stabilities, outstanding mechanical and electrical properties; therefore, all kinds of aromatic PIs have been widely used in the fields of adhesives, coatings, films, fibers, composite matrix resins, as well as microelectronic materials.[1–6] However, the mechanical, thermal, and adhesion properties of PIs are in need of further improvement for applications in advanced microelectronic field.

As we know, crystallization, interactions, and orientation are three vital factors for enhancing mechanical properties of polymers. Aromatic PIs exhibit semicrystalline or amorphous structure, which is influenced by their chemical structure and thermal imidization process.[7,8] Zhuang *et al.*[9] investigated structure–property relationships of co-PI films containing benzoxazole and benzimidazole moieties. Their results indicated the introduction of benzoxazole moieties into the PI backbone enhanced the mechanical properties due to the improvement of the crystallinity.[9] Hydrogen bonding, as the strongest physical interaction, is a useful way to improve the mechanical properties of polymer.[10] However, PIs generally show no hydrogen bonding interactions after fully imidization. In recent years, hydrogen bond interactions have been introduced into PI's main chain by means of benzimidazole groups.[11–18] The benzimidazole moiety with both proton acceptor (C═N) and proton donor (—NH—) would exhibit strong hydrogen bonding interactions with carbonyl functionalities,[15,19,20] which brings about an undesirable Tg and tensile strength increase for the corresponding PIs.[13,21] Moreover, PI films with rigid chains would exhibit remarkable spontaneous in-plane orientation induced by

Additional Supporting Information may be found in the online version of this article.

thermal imidization,[22–24] which leads to a decrease in the linear coefficient of thermal expansion (CTE) and an increase in mechanical properties.[24,25] However, the dominant factor for the improvement of mechanical properties remains unclear.

What is more, PIs containing heterocyclic moiety, which is due to their high mechanical properties, outstanding thermal properties, and good adhesion to metal,[26,27] are receiving more and more attention and becoming an important type of high-performance PI materials in recent years.[14,15,28–36] Thus, three PI films, containing the benzoxazole, benzimidazole, and pyrimidine moieties, respectively, were chosen to discuss the structure–property relationships. The difference of in-plane orientation, molecular packing, and mechanical properties in three PIs was examined. Hydrogen bonding interactions, the degree of crystallization, and orientation factors were discussed in detail in order to study the dominant factor for the improvement of mechanical properties. This work is helpful to further understanding structure–property relationships of PIs and would provide a theoretical guidance for designing high performance PIs.

EXPERIMENTAL

Materials

N-Methyl-2-pyrrolidone (NMP) was obtained from Shanghai Qunli Chemical Company in shanghai, and was distilled over P_2O_5 under reduced pressure before use. 3,3′,4,4′-Biphenyltetracarboxylic dianhydride (BPDA) was obtained from Changzhou Sunlight Medical Raw Material Co., Ltd. (Changzhou, China) and was dried in an oven at 200 °C for 10 h before use. 5(6)-Amino-2-(4-aminobenzene)benzoxazole (BOA) and 5(6)-amino-2-(4-aminobenzene)benzimidazole (PABZ) were obtained from Changzhou Sunlight Medical Raw Material Co., Ltd., and used as received. 2,5-Bis(4-aminophenyl)pyrimidine (PRM) was synthesized and purified according to the procedure published in Ref. 35 and dried thoroughly under vacuum prior to use.

Synthesis of Poly(amic acid)

The solvent (NMP) was added into 50-mL three-neck round flask under dried nitrogen atmosphere. Then, a certain amounts of diamine were added into NMP under stirring. After the diamine dissolved or dispersed in NMP, the equimolar amounts of dianhydride were added. For example, 1.8044 g (0.008055 mol) PABZ was dissolved in 30 ml NMP, and then 2.3683 g (0.008055 mol) BPDA was added. The mixture was stirred in a 50-mL three-neck round flask at room temperature for 50 h. A viscous solution of BPDA/PABZ with a solid content of 12 wt % was obtained. The solid content of obtained BPDA/BOA and BPDA/PRM PAA solutions is 14 and 12%, respectively. In addition, the intrinsic viscosity of BPDA/PABZ, BPDA/BOA, and BPDA/PRM PAA solutions is 2.8, 2.6, and 2.5.

Preparation of PI Films

The three PAAs were first cast onto clean and dry glass plates and were subsequently imidized by heating at 80 °C for 1 h, 160 °C for 1 h, 220 °C for 1 h, and 300 °C for 1 h in a vacuum baking oven. Then the PI films were further annealed at 400 °C for 30 min. After the thermal treatment, the films were removed from the glass plates by immersing into water and then were dried at 100 °C for 4 h. The thicknesses of the PI films obtained were 10–15 μm. The three PAAs were also spin-coated onto quartz plate and were subsequently imidized by heating at 80 °C for 1 h, 160 °C for 1 h, 220 °C for 1 h, 300 °C for 1 h, and 400 °C for 0.5 h in a vacuum baking oven. The thicknesses of spin-coated films were 10 ± 2 μm. Figure 1 shows the synthetic process and the chemical structure of the PIs.

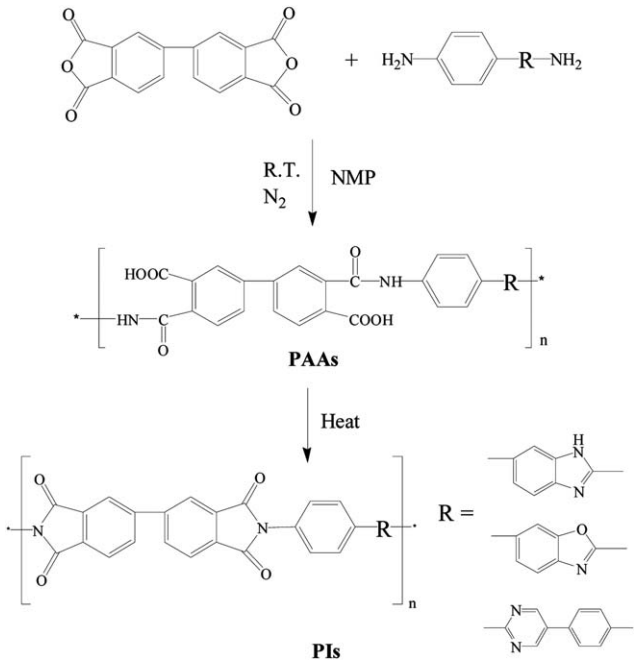

Figure 1. Scheme of the preparation process of polyimide.

Characterization

Mechanical properties such as the tensile strength and initial modulus elongation at break of the PI films were measured on Instron Modle 5567 with a strain rate of 5 mm/min. The specimens were 10-mm width and 8-cm long, and the fixture span was 20 mm.

Wide angle X-ray diffraction (WAXD) measurements were performed at room temperature, using a Rigaku vertical diffractometer (Model Ultima IV). The Cu Kα radiation operated at 40 kV and 40 mA. The *d*-spacing of each diffraction peak was calculated using the Bragg equation. Curve-fitting deconvolution of the WAXD spectra was performed using Origin 8.5 Software to separate crystallization and amorphous contributions. The peaks were fitted assuming in Gaussian type. The crystallinity (X_C) was calculated with eq. (1) following the peak fitting.[15]

$$X_C = \frac{A_c}{A_c + A_a} \times 100\% \quad (1)$$

A_c is crystallization peak area, and A_a is the amorphous peak area.

Small angle X-ray scattering (SAXS) experiments were performed using a NanoSTAR-U (BRUKER AXS Inc., Madison, Wisconsin, USA) with Cu Kα radiation ($\lambda = 0.154$ nm). The generator was operated at 40 kV and 650 μA. Two-dimensional SAXS patterns were obtained using a HI-STAR detector. The sample to detector distances was 1074 mm. The effective scattering vector q ($q=(4\pi/\lambda)\sin\theta$, where 2θ is the scattering angle) at this distance ranges from 0.044 to 2.0 nm^{-1}. Fourier

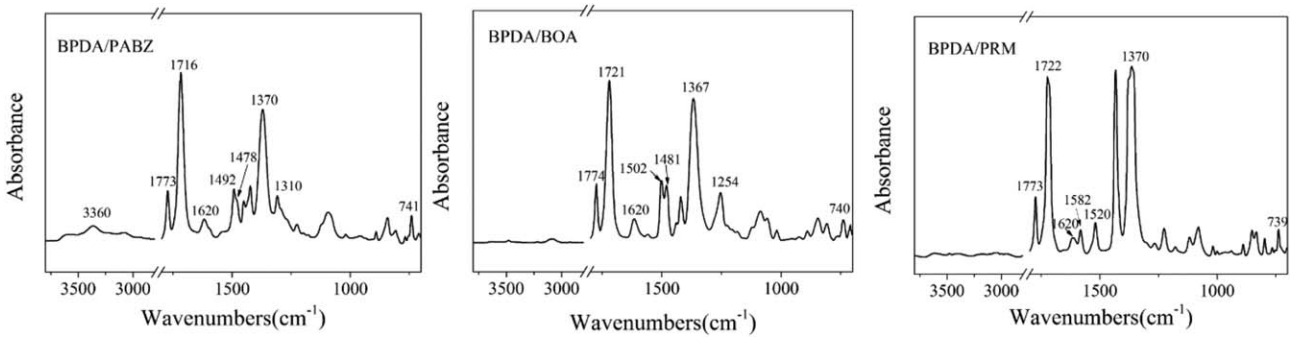

Figure 2. The FTIR profiles of BPDA/PABZ, BPDA/BOA, and BPDA/PRM PI films.

transform infrared (FTIR) spectra of PI films were measured at a Nicolet Magna 650 spectroscope in the range of 4000–400 cm^{-1}.

Polarized ATR-FTIR spectra of peeled PI films were measured using a Nicolet 560 Fourier on the atmospheric sides transform spectrometer attached with Spectra-Tech Thunderdome single reflection ATR attachment (incident angle is 45°) and aluminum wire-grid ZnSe polarizer. The IRE in the ATR attachment is made of germanium crystal with a refractive index of 4.0. For polarized ATR-FTIR measurement, the polarized angle varied from 0 to 180°, and a series of spectra were recorded by every 15°. Polarized ATR-FTIR spectra were obtained using polarized IR radiation with different electric vectors.

In-plane (n_{TE}) and out-of-plane refractive indices (n_{TM}) were measured using a prism-coupler (Model 2000; Metricon, Pennington, New Jersey, USA) at a wavelength of 1538 nm. The experimental errors of the refractive indices are smaller than 0.001.

Molecular simulation was determined with Dmol3 software embedded in Material Studio 4.0 (Accelrys Software Inc., San Diego, CA, USA) package. Molecules were relaxed through NVT molecular dynamics, the time evolution of chain conformations, up to 1000 ps with time steps of 0.0002 ps. Simulation temperatures of 300 and 800 K were employed in order to further relax local hot-spots and to allow the system to come to thermal equilibrium.

The lateral (in-plane) CTE was measured over the range of 40–250 °C with a load of 5 cN under a N_2 gas flow using TMA-Q400 with a tension probe. The ramping rate is 5.0 °C/min. Before the measurement, the film specimens were heated to 250 °C with a ramping rate of 10.0 °C/min, soaked for 10 min at 250 °C, and then cooled down to 40 °C with a cooling rate of 10.0 °C/min, in order to remove residual stress in the films. CTE was averaged over the range of 100–200 °C. The gauge length was 15.6 mm, and the width of film strips was 3 mm.

RESULTS AND DISCUSSION

Chemical Structure and Hydrogen Bonding Interactions

The FTIR results of three PI samples are shown in Figure 2. In the region of 1800∼700 cm^{-1}, the characteristic absorption bands of the imide ring are observed at about 1770 (the symmetric stretching of the imide carbonyls $\nu s_{C=O}$), 1720 (the asymmetric stretching of the imide carbonyls $\nu as_{C=O}$), 1370 (the stretching of C–N νs_{C-N}), and 740 cm^{-1}.[37,38] The characteristic absorption bands at 1492–1520 cm^{-1} and at about 1620 cm^{-1} are assigned to C–C stretching vibration of 1,4-C_6H_4 in backbone and C=C stretching vibration of benzene ring, respectively.[39] Meanwhile, the characteristic absorption bands of PAAs (around 1650 cm^{-1} for amide-I band and 1550 cm^{-1} for amide-II band) are not identified. Those results indicate that the three PI films were successfully prepared, and high imidization degree was obtained.[40,41] Moreover, the characteristic absorptions of benzimidazole at 3360 (N–H stretching) and 1308 cm^{-1} (imidazole ring breathing mode[9]) are shown in poly(benzoxazole-imide) (BPDA/PABZ). Poly(benzimidazole-imide) (BPDA/BOA) film shows the characteristic absorptions of benzoxazole at 1254 cm^{-1} (Ar–C–O asymmetric stretching[9]), suggesting that the benzoxazole moiety has been successfully incorporated into the main chains. The absorption bands at 1582 cm^{-1} correspond to C=N stretching of pyrimidine moiety in poly(pyrimidine-imide) (BPDA/PRM) film. What is more, the asymmetric stretching of the imide carbonyls $\nu as_{C=O}$ at about 1720 cm^{-1} is sensitive to interactions.[2] The wavenumber of $\nu as_{C=O}$ of BPDA/PABZ PI is 1716 cm^{-1}, which is lower than those of BPDA/BOA (1721 cm^{-1}) and BPDA/PRM (1722 cm^{-1}) PI. Moreover, in our previous paper,[15] we analyzed the formation of hydrogen-bonding interaction in BPDA/PABZ PI by comparing the wavelength number shifts of the C=O bond in the imide rings. Thus, hydrogen bonding interactions are formed in BPDA/PABZ PI.

Aggregation Structure and Morphology

The out-of-plane WAXD profiles of three PI films in reflection pattern are illustrated in Figure 3. Three diffraction peaks at $2\theta = 14.6$, 23.9, and 26.4° and five diffraction peaks at $2\theta = 14.4$, 16.9, 22.1, 24.2, and 26.4° are observed for BPDA/PABZ and BPDA/BOA PI films, respectively. As mentioned in previous articles,[9,16] the peak of 14.6° (2θ) is correspond to the "side to side" packing of benzoxazole/benzimidazole rings, and the peak of 24.0° (2θ) is assigned to the "π–π stacking" of aromatic of heterocyclic rings. However, there are only two diffraction peaks at $2\theta = 21.1$ and 25.3° in BPDA/PRM PI. Those results indicate that three PI films show regularly lateral ordered structure, and the lateral order in the direction of film thickness is the increasing order: BPDA/PRM < BPDA/PABZ < BPDA/BOA. The larger lateral order of BPDA/BOA and BPDA/PABZ PIs may be due to the bigger coplanar benzoxazole and benzimidazole rings. In addition, the degree of crystallization (X_C) of three PIs

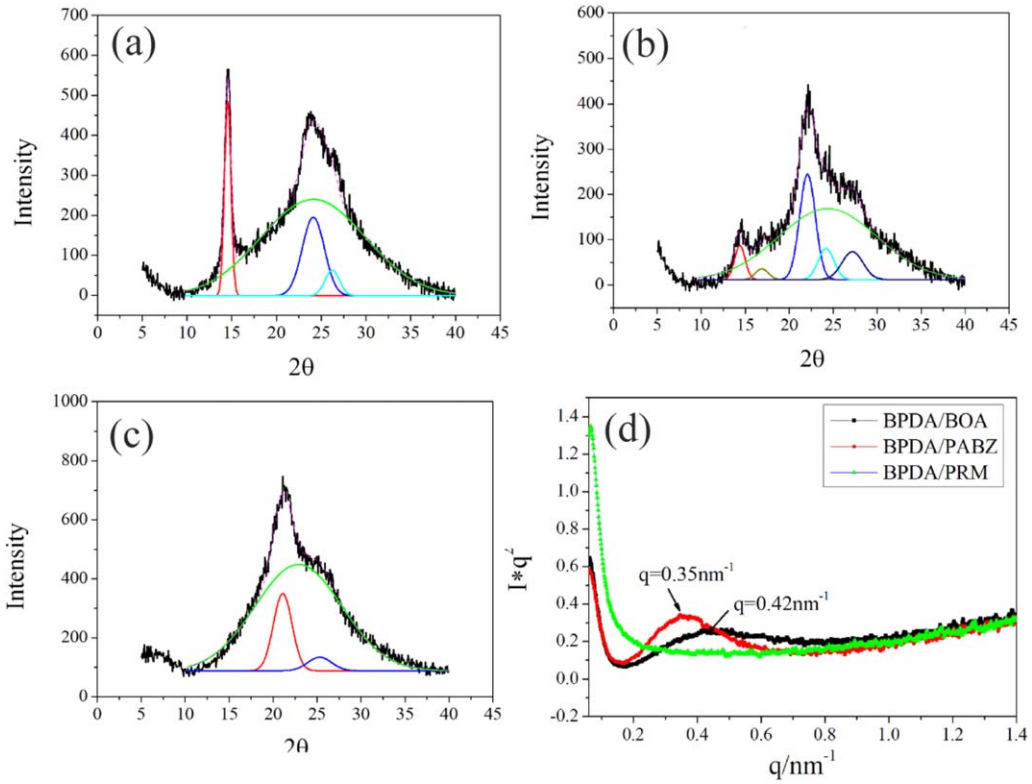

Figure 3. (a) The WAXD profiles and peak fitting of BPDA/PABZ PI; (b) the WAXD profiles and peak fitting of BPDA/BOA PI; (c) the WAXD profiles and peak fitting of BPDA/PRM PI; and (d) the SAXS patterns of three PI films. [Color figure can be viewed in the online issue, which is available at wileyonlinelibrary.com.]

was calculated by peak fitting, and the results are shown in Table I. The values of X_C of BPDA/PABZ, BPDA/BOA, and BPDA/PRM PI are 24, 36, and 15%, respectively.

SAXS measurement was used to characterize the morphology of PI films. The Lorentz-corrected SAXS[42] curves of samples are shown in Figure 3(d). The Lorentz-corrected SAXS curves of BPDA/PABZ and BPDA/BOA PI films exhibit a peak at 0.35 and 0.42 nm^{-1}, respectively. Those results suggest that the periodical lamellar structure is formed in BPDA/PABZ and BPDA/BOA PI films, which was also reported by other researchers.[17,34] A long period (L) can be calculated from the equation $L = 2\pi/q_{max}$, where q_{max} is the peak value in the Lorentz-corrected SAXS plot.[42] For semicrystalline polymer, lamellar thickness (L_M) can be calculated by using the equation $L_M = X_C \times L$, where X_C is the crystallinity of polymer.[43] Crystallinity and lamellar thickness of PI samples are summarized in Table I. Lamellar thickness of BPDA/PABZ and BPDA/BOA PI films shows 4.3 and 5.4 nm, respectively. However, no peaks are observed in the SAXS curve of BPDA/PRM PI films, which suggests that no periodical lamellar structure exists in BPDA/PRM PI sample.

In-Plane Orientation

The polarized ATR-FTIR spectra of three casting PI films are shown in Figure S1 in supporting information. The peak intensities at about 1720 and 1500 cm^{-1} change regularly with the increase of polarization angle from 0 to 90°. Figure 4(a) and (b) shows polar diagrams of absorbance of peaks at about 1720 and 1500 cm^{-1} as a function of the angle of polarization of incident polarized light. They are obtained using linearly polarized IR spectroscopy: (1) ~1720 cm^{-1} (νas(C=O), C=O asymmetric stretching vibration of imide ring) and (2) ~1500 cm^{-1} (ν(C–C), C–C stretching vibration of 1,4-C_6H_4 in backbone). The polar diagrams of 1720 cm^{-1} of three PI films exhibit a maximum intensity of absorbance peak at the direction 90 and 270° and a minimum intensity at the direction 0 and 180°. Those results indicate that the transition moment of νas(C=O) orients parallel to the direction of the Z-axial. Since the transition moment of νas(C=O) is also perpendicular to imide rings, as shown in Figure 4(c), it means that imide rings of PIs favorably orient parallel to the plane of films. In addition, the transition moments of ν_{C-C} are parallel to the direction of the biphenyl group and the polar diagrams of ν_{C-C} (~1500 cm^{-1}) of three PI films exhibit a maximum intensity of absorbance peak at the direction 0 and 180° and a minimum intensity at the direction 90 and 270°. So it can be concluded that the PI molecular backbones show higher degree of in-plane orientation, which mainly resulted from the rigid-rod molecular structures.[39,44]

Table I. Crystallinity and lamellar thickness of PI samples

PIs	X_C (%)	L (nm)	L_M (nm)
BPDA/PABZ	24	17.9	4.3
BPDA/BOA	36	15.0	5.4
BPDA/PRM	15	—	—

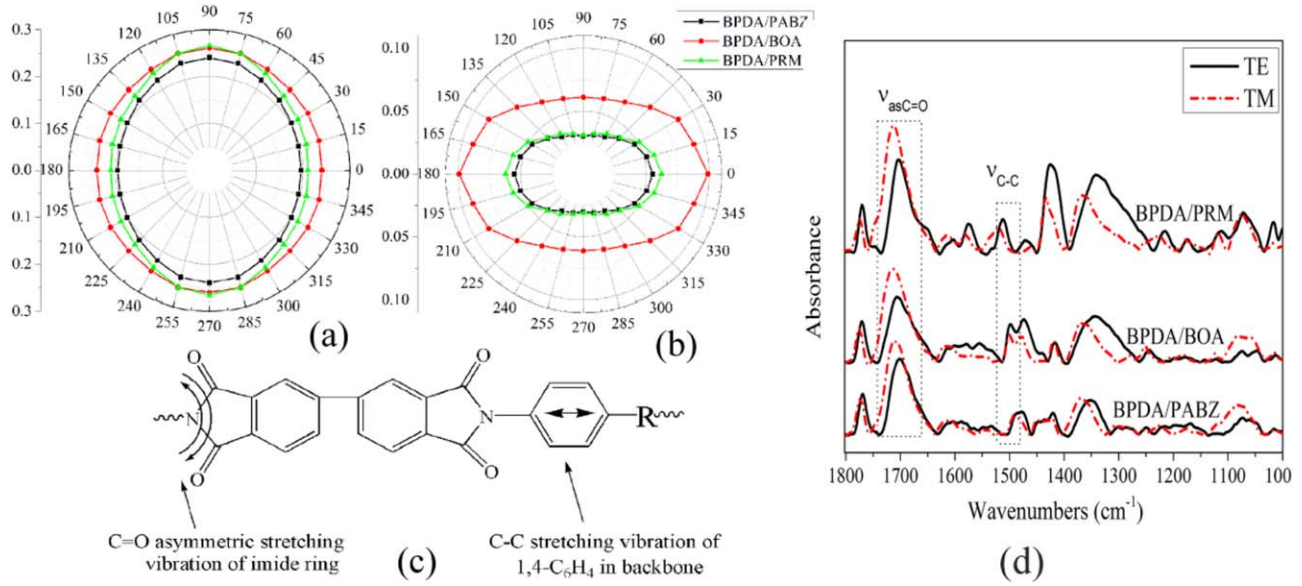

Figure 4. Polar diagrams of absorbance of peaks for casting films at different positions as a function of the angle of polarization of incident polarized light, obtained using linearly polarized IR spectroscopy: (a) 1720 cm^{-1} (C=O asymmetric stretching vibration of imide ring) and (b) 1490~1520 cm^{-1} (C–C stretching vibration of 1,4-C_6H_4 in backbone); (c) vibration modes and the directions of transition moments for PIs; and (d) the obtained ATR/FT-IR spectra of BPDA/PABZ, BPDA/BOA, and BPDA/PRM spin-coated PI films for TE- and TM-polarized incident light. [Color figure can be viewed in the online issue, which is available at wileyonlinelibrary.com.]

In addition, during the solution casting process, PAA preorientation was induced and orientation at the stage of casting PAAs also appreciably influenced the final in-plane orientation of PI films. In order to accurately calculate in-plane orientation coefficients, we should make sure that orientation and refractive indices at *X* direction and at *Y* direction are the same. So three PAA films were spin coated, and there was no difference of orientation and refractive indices between *X* direction and *Y* direction for spin-coated films. The thicknesses of spin-coated films were 10 ± 2 μm. From the previous results,[45,46] when the thickness of PI film was about 10 μm, the effect of film thickness on chain orientation can be negligible. Thus, the films near the air side were chosen to calculate orientation. The polarized ATR-FTIR spectra of spin-coated PI films near the air side are shown in Figure 4(d) and in-plane absorbance (A_{TE}) and out-of-plane absorbance (A_{TM}) can be obtained from Figure 4(d). In addition, in-plane (n_{TE}) and out-of-plane (n_{TM}) refractive indices were tested and shown in Table II. A schematic figure for the ATR/FT-IR spectroscopy and fundamental principle to calculate orientation factors were shown in Refs. 44,46, and 47. The in-plane orientation coefficients P_{200} can be calculated by the following equations[44,46]:

$$\frac{k_{TM}-k_{TE}}{2k_{TE}+k_{TM}} = P_{200}(\theta_m)\times P_{200} + 2(P_{200}(\theta_m)-1)\times P_{202} \quad (2)$$

$$P_{200}(\theta_m) = \frac{1}{2}(3\cos\theta_m - 1) \quad (3)$$

where k_{TE} and k_{TM} are the extinction coefficients and were calculated from the degrees of absorptions A_{TE} and A_{TM} for the parallel band at about 1500 cm^{-1} (ν(C–C)) and perpendicular band at about 1720 cm^{-1} (ν(C=O)).[37,44,46,48,49] θ_m is the angle between the chain direction of PI and the transition moment of the corresponding absorption band at IR. For example, $\theta_m = 0°$ ($P_{200}(\theta_m) = 1$) for the parallel bands and $\theta_m = 90°$ ($P_{200}(\theta_m) = -0.5$) for the perpendicular bands.[46] Since the average orientation of PI chains in spin-coated films is generally along the film plane, as the value of P_{200} is close to −0.5, the in-plane orientation to the film planes is larger. The angle θ_m between the PI chain direction and the ν(C–C) skeletal vibrations is 0° ($P_{200}(\theta_m) = 1$) for three fully rod-like PIs.[46] On the other side, the angle θ_m between the PI chain direction and ν(C=O) asymmetric vibrations is 90°, which means $P_{200}(\theta_m) = -0.5$.[46] Thus, in-plane orientation coefficients P_{200} were calculated from the absorption strength of skeletal vibration of 1,4-disubstituted benzene (~1500 cm^{-1}) and that of C=O asymmetric stretching vibration of imide ring (~1720 cm^{-1}). The results are listed in Table II. The values of P_{200} of BPDA/PABZ, BPDA/BOA, and BPDA/PRM PI spin-coated films are −0.296, −0.315, and −0.331. The values of P_{200} approach to −0.5 as the degree of orientation to the film plane becomes larger. So the degree of in-plane orientation is in increasing order BPDA/PABZ < BPDA/BOA < BPDA/PRM.

Why does BPDA/PRM PI film show the highest in-plane orientation? Hasegawa *et al.* demonstrated that spontaneous molecular orientation of PI was induced by thermal imidization.[22–24]

Table II. In-plane (n_{TE}), out-of-plane refractive indices (n_{TM}), and in-plane orientation coefficients (P_{200}) for the three spin-coated polyimide films

Polyimides	n_{TE}	n_{TM}	P_{200}
BPDA/PABZ	1.7216	1.5942	−0.296
BPDA/BOA	1.7245	1.5915	−0.315
BPDA/PRM	1.7320	1.5833	−0.331

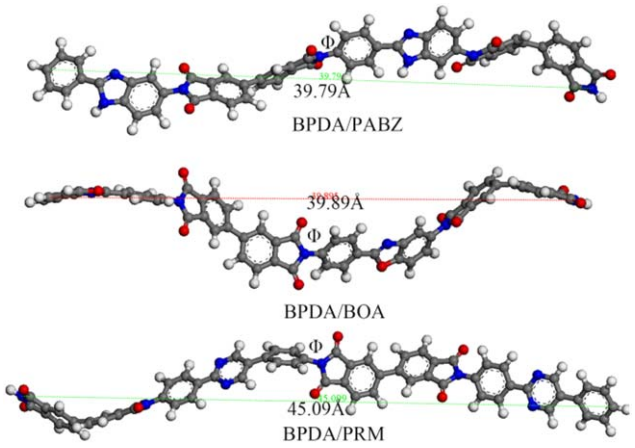

Figure 5. The chemical structure of the dimer models of PIs. [Color figure can be viewed in the online issue, which is available at wileyonlinelibrary.com.]

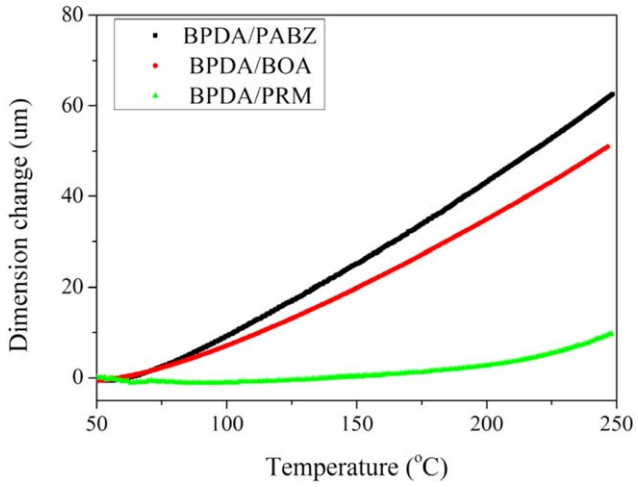

Figure 6. TMA curves of three PI films. [Color figure can be viewed in the online issue, which is available at wileyonlinelibrary.com.]

PI films with more rigid chains would exhibit higher in-plane orientation, and a certain extent of molecular mobility was required for the improvement of the in-plane orientation.22 Figure 5 depicts the optimized molecular structures of the dimer models. The mean square end-to-end distance (R_2) of dimer models of BPDA/PABZ, BPDA/BOA, and BPDA/PRM PIs are 39.79, 39.89, and 45.09 Å, respectively. The chain rigidity is in increasing order BPDA/PABZ ≈ BPDA/BOA < BPDA/PRM. The highest rigidity of BPDA/PRM PI leads to the highest degree of in-plane orientation. BPDA/PABZ and BPDA/BOA PIs show the similar chemical structure and rigidity, but BPDA/BOA PI exhibits higher in-plane orientation than that of BPDA/PABZ PI. The hydrogen bonding interactions in BPDA/PABZ PI restrict chain motion[15] and would hinder spontaneous molecular orientation induced by thermal imidization.

In-Plane CTE

The in-plane CTE values were directly measured by the TMA instrument, and CTE was averaged over the range of 100–200 °C. The results are shown in Figure 6(a) and Table III. The in-plane CTE values of three PI films are in the range of 2.3–21.3 ppm/°C and are in increasing order BPDA/PRM < BPDA/BOA < BPDA/PABZ. In-plane CTE was found to be significantly affected by the variation of chain orientation and the in-plane CTE decreased considerably when the degree of in-plane chain orientation increase.[45,50,51] Thus, the lowest lateral CTE value of BPDA/PRM PI film also indicates the highest in-plane orientation, which is in accordance with the results of the polarized ATR-FTIR.

Mechanical Properties

Mechanical properties of the PI films are summarized in Table III. The films exhibited the tensile strength of 254.1–367.6 MPa, the elongation at break of 32.0–45.3%, and the elasticity modulus of 4633.1–5398.2 MPa, indicating the high mechanical properties due to the introduction of rigid heteroaromatic moieties to the PI main chains.[9] Besides, the tensile strength and elasticity modulus are in increasing order BPDA/PABZ < BPDA/BOA < BPDA/PRM. Generally, better mechanical properties of the polymers would be obtained with higher intrinsic viscosity, crystallinity, in-plane orientation, and intermolecular interactions. From the previous results, mechanical properties of PIs were not mainly affected by the intrinsic viscosity.[2,9] BPDA/PRM PI shows no hydrogen bonding interactions and low degree of crystallization ($X_C = 15\%$). Thus, the highest in-plane orientation ($P_{200} = -0.331$) mainly leads to the highest tensile strength and elasticity modulus. BPDA/BOA PI films possess the highest degree of crystallization ($X_C = 36\%$) and the second highest in-plane orientation ($P_{200} = -0.315$). Their mechanical properties rank only second to that of BPDA/PRM PI. BPDA/PABZ PI films show the lowest tensile strength and initial modulus even though strong hydrogen bonding interactions are formed in macromolecular chains. The lowest in-plane orientation ($P_{200} = -0.296$) and the second highest degree of crystallization ($X_C = 25\%$) are found in BPDA/PABZ PI. From the above analysis, beneficial to the improvement of mechanical properties is mainly derived from three factors, and the order of influence extent is hydrogen bonding interactions < degree of crystallization < in-plane orientation. It is concluded that in-plane orientation is the dominant factor for the enhancement of mechanical properties of PI film.

Table III. Mechanical properties and CTE value of the polyimide films

Polyimides	Tensile strength (MPa)	Elasticity modulus (MPa)	Elongation at break (%)	CTE (ppm/°C)
BPDA/PABZ	254.6 ± 12.3	4633.1 ± 35.2	36.8 ± 4.5	21.3
BPDA/BOA	323.4 ± 16.4	4822.9 ± 31.2	45.3 ± 6.8	17.8
BPDA/PRM	367.6 ± 19.1	5398.2 ± 45.5	32.0 ± 5.7	2.3

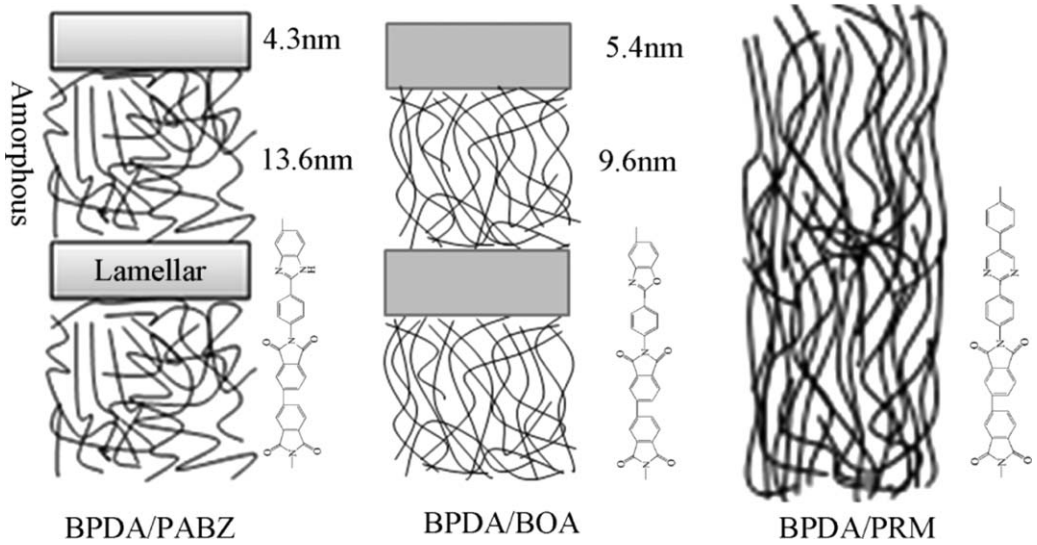

Figure 7. The sketch of two hypothetical structure models for the PI films.

Two Structure Models for PI Films

The dominant effect of in-plane orientation on the mechanical properties is further confirmed as following. From the above results, BPDA/PABZ and BPDA/BOA PI films show higher degree of crystallization and periodical lamellar structure. The corresponding lamellar thickness is 4.3 and 5.4 nm for BPDA/PABZ and BPDA/BOA PIs, respectively. However, BPDA/PRM PI film shows lower degree of crystallization and no periodical lamellar structure, but the overall orientation of BPDA/PRM PI chain is very high. Based on the above analysis, the sketch of two hypothetical structure models for the PI films is proposed and shown in Figure 7. The one is lamellar structure for BPDA/PABZ and BPDA/BOA PIs. The other possesses no lamellar structure with high in-plane orientation of macromolecular chains for BPDA/PRM PI. High overall orientation and low crystallinity imply homogeneous liquid-crystalline-like ordered domains, which are favor of stress transfer and result in the enhancement of mechanical properties.

CONCLUSIONS

Three PI films, containing the benzoxazole, benzimidazole, and pyrimidine moieties, were chosen to discuss the structure–property relationship. The incorporation of big coplanar benzimidazole or benzoxazole moieties into PI main chain would increase crystallization and form periodical lamellar structure. BPDA/PRM PI containing pyrimidine moiety shows no peak in SAXS, indicating the absence of lamellar structure. In-plane orientation P_{200} of macromolecular was calculated from in-plane and out-of-plane polarized ATR-FTIR and refractive indices. The P_{200} values of spin-coated BPDA/PABZ, BPDA/BOA, and BPDA/PRM PIs are −0.296, −0.315, and −0.331, respectively. The highest degree of in-plane orientation for BPDA/PRM PI film is due to highest rigidity. In contrast, the hydrogen bonding interactions in BPDA/PABZ PI restrict chain motion and hinder spontaneous molecular orientation induced by thermal imidization. The highest in-plane orientation of BPDA/PRM PI leads to highest tensile strength (367.6 MPa) and initial modulus (5398.2 MPa). Due to the highest crystallinity and the second highest in-plane orientation (P_{200} = −0.315), mechanical properties of BPDA/BOA PI films rank only second to that of BPDA/PRM PI films. BPDA/PABZ PI films show the lowest tensile strength and initial modulus even though strong hydrogen bonding interactions are formed in macromolecular chains. Those results indicated that the order of influence extent for mechanical properties is hydrogen bonding interactions < degree of crystallization < in-plane orientation. Moreover, two structure models for PIs are proposed to further confirm the in-plane orientation dominant effect. The one was lamellar structures with lamellar thickness 4.3 and 5.4 nm for BPDA/PABZ and BPDA/BOA PIs, respectively. The other was high in-plane orientation of macromolecular chains without lamellar structures for BPDA/PRM PI. High overall orientation and low crystallinity imply homogeneous liquid-crystalline-like ordered domains, which are mainly formed in the macromolecular chain of BPDA/PRM PI, are favor of stress transfer, and result in the enhancement of mechanical properties.

ACKNOWLEDGMENTS

This work was financially supported by the National Natural Science Foundation of China (Grant No. 51573105) and State Key Laboratory of Polymer Materials Engineering (Grant No. sklpme 2014-2-04). The authors acknowledge Analytical & Testing Centre of Sichuan University, People's Republic of China, for characterization.

REFERENCES

1. Sroog, C. *Prog. Polym. Sci.* **1991**, *16*, 561.
2. Luo, L.; Zheng, Y.; Huang, J.; Li, K.; Wang, H.; Feng, Y.; Wang, X.; Liu, X. *J. Appl. Polym. Sci.* **2015**, *132*, DOI: 10.1002/app.42001.
3. Marashdeh, W. F.; Longun, J.; Iroh, J. O. *J. Appl. Polym. Sci.* **2016**, *133*, DOI: 10.1002/app.43684.
4. Li, B.; Wu, Z.; Lin, L. *J. Appl. Polym. Sci.* **2016**, *133*, DOI: 10.1002/app.43680.

5. Feng, Y.; Luo, L. B.; Huang, J.; Li, K.; Li, B.; Wang, H.; Liu, X. *J. Appl. Polym. Sci.* **2016**, *133*, DOI: 10.1002/app.43677.
6. Luo, L.; Wang, Y.; Zhang, J.; Huang, J.; Feng, Y.; Peng, C.; Wang, X.; Liu, X. *Macromol. Mater. Eng.* **2016**. DOI: 10.1002/mame.201600113.
7. Wang, Y.; Yang, Y.; Jia, Z.; Qin, J.; Gu, Y. *Polymer* **2012**, *53*, 4157.
8. Ree, M.; Kim, K.; Woo, S.; Chang, H. *J. Appl. Phys.* **1997**, *81*, 698.
9. Zhuang, Y.; Liu, X.; Gu, Y. *Polym. Chem.* **2012**, *3*, 1517.
10. Luo, L.; Pang, Y.; Jiang, X.; Wang, X.; Zhang, P.; Chen, Y.; Peng, C.; Liu, X. *J. Polym. Res.* **2012**, *19*, 1.
11. Gao, G.; Dong, L.; Liu, X.; Ye, G.; Gu, Y. *Polym. Eng. Sci.* **2008**, *48*, 912.
12. Liu, X.; Gao, G.; Dong, L.; Ye, G.; Gu, Y. *Polym. Adv. Technol.* **2009**, *20*, 362.
13. Song, G.; Zhang, Y.; Wang, D.; Chen, C.; Zhou, H.; Zhao, X.; Dang, G. *Polymer* **2013**, *54*, 2335.
14. Dong, J.; Yin, C.; Zhang, Z.; Wang, X.; Li, H.; Zhang, Q. *Macromol. Mater. Eng.* **2014**, *299*, 1170.
15. Luo, L.; Yao, J.; Wang, X.; Li, K.; Huang, J.; Li, B.; Wang, H.; Liu, X. *Polymer* **2014**, *55*, 4258.
16. Zhuang, Y.; Gu, Y. *J. Polym. Res.* **2012**, *19*, 1.
17. Yin, C.; Dong, J.; Tan, W.; Lin, J.; Chen, D.; Zhang, Q. *Polymer* **2015**, *75*, 178.
18. Zhang, M.; Niu, H.; Lin, Z.; Qi, S.; Chang, J.; Ge, Q.; Wu, D. *Macromol. Mater. Eng.* **2015**, *300*, 1096.
19. Ahn, T. K.; Kim, M.; Choe, S. *Macromolecules* **1997**, *30*, 3369.
20. Guerra, G.; Choe, S.; Williams, D. J.; Karasz, F. E.; MacKnight, W. J. *Macromolecules* **1988**, *21*, 231.
21. Xia, Q.; Liu, J.; Dong, J.; Yin, C.; Du, Y.; Xu, Q.; Zhang, Q. *J. Appl. Polym. Sci.* **2013**, *129*, 145.
22. Hasegawa, M.; Matano, T.; Shindo, Y.; Sugimura, T. *Macromolecules* **1996**, *29*, 7897.
23. Hasegawa, M.; Shindo, Y.; Sugimura, T.; Yokota, R.; Kochi, M.; Mita, I. *J. Polym. Sci. B: Polym. Phys.* **1994**, *32*, 1299.
24. Ebisawa, S.; Ishii, J.; Sato, M.; Vladimirov, L.; Hasegawa, M. *Eur. Polym. J.* **2010**, *46*, 283.
25. Ree, M.; Chu, C. W.; Goldberg, M. J. *J. Appl. Phys.* **1994**, *75*, 1410.
26. Chung, I. S.; Park, C. E.; Ree, M.; Kim, S. Y. *Chem. Mater.* **2001**, *13*, 2801.
27. Yu, J.; Ree, M.; Shin, T.; Wang, X.; Cai, W.; Zhou, D.; Lee, K. W. *Polymer* **2000**, *41*, 169.
28. Liu, J.; Zhang, Q.; Xia, Q.; Dong, J.; Xu, Q. *Polym. Degrad. Stab.* **2012**, *97*, 987.
29. Zhang, P.; Chen, Y.; Li, G.; Luo, L.; Pang, Y.; Wang, X.; Peng, C.; Liu, X. *Polym. Adv. Technol.* **2012**, *23*, 1362.
30. Yin, C.; Dong, J.; Zhang, D.; Lin, J.; Zhang, Q. *Eur. Polym. J.* **2015**, *67*, 88.
31. Song, G.; Zhang, X.; Wang, D.; Zhao, X.; Zhou, H.; Chen, C.; Dang, G. *Polymer* **2014**, *55*, 3242.
32. Wang, Y. *High Perform. Polym.* **2014**, *26*, 455.
33. Sukhanova, T.; Baklagina, Y. G.; Kudryavtsev, V.; Maricheva, T.; Lednický, F. *Polymer* **1999**, *40*, 6265.
34. Ma, X.; Kang, C.; Chen, W.; Jin, R.; Guo, H.; Qiu, X.; Gao, L. *J. Polym. Sci. A: Polym. Chem.* **2016**, *54*, 570.
35. Xia, A.; Guo, H.; Qiu, X.; Ding, M.; Gao, L. *J. Appl. Polym. Sci.* **2006**, *102*, 1844.
36. Xia, A.; Lü, G.; Qiu, X.; Guo, H.; Zhao, J.; Ding, M.; Gao, L. *J. Appl. Polym. Sci.* **2006**, *102*, 5871.
37. Ishida, H.; Wellinghoff, S. T.; Baer, E.; Koenig, J. L. *Macromolecules* **1980**, *13*, 826.
38. Ishida, H.; Huang, M. *J. Polym. Sci. B: Polym. Phys.* **1994**, *32*, 2271.
39. Wang, X.; Zhang, P.; Chen, Y.; Luo, L.; Pang, Y.; Liu, X. *Macromolecules* **2011**, *44*, 9731.
40. Shin, T. J.; Ree, M. *J. Phys. Chem. B* **2007**, *111*, 13894.
41. Shin, T. J.; Ree, M. *Langmuir* **2005**, *21*, 6081.
42. Huang, J.; Li, K.; Luo, L.; Wang, H.; Wang, X.; Feng, Y.; Liu, X. *Cryst. Growth Des.* **2015**, *15*, 2072.
43. Zhou, H.; Wilkes, G. *Polymer* **1997**, *38*, 5735.
44. Matsuda, S. I.; Ando, S. *J. Polym. Sci. B: Polym. Phys.* **2003**, *41*, 418.
45. Jo, B. W.; Ahn, K. H. *J. Polym. Sci. B: Polym. Phys.* **2014**, *52*, 848.
46. Terui, Y.; Matsuda, S. I.; Ando, S. *J. Polym. Sci. B: Polym. Phys.* **2005**, *43*, 2109.
47. Everall, N. J.; Bibby, A. *Appl. Spectrosc.* **1997**, *51*, 1083.
48. Jarvis, D.; Hutchinson, I.; Bower, D.; Ward, I. *Polymer* **1980**, *21*, 41.
49. Ishida, H.; Huang, M. *Spectrochim. Acta A* **1995**, *51*, 319.
50. Dabral, M.; Xia, X.; Gerberich, W.; Francis, L.; Scriven, L. *J. Polym. Sci. B: Polym. Phys.* **2001**, *39*, 1824.
51. Jo, B. W.; Ahn, K. H.; Lee, S. J. *Polymer* **2014**, *55*, 5829.